PAPER

Signal-amplifying nanoparticle/hydrogel hybrid microarray biosensor for metal-enhanced fluorescence detection of organophosphorus compounds

Biofabrication

PAPER

Signal-amplifying nanoparticle/hydrogel hybrid microarray biosensor for metal-enhanced fluorescence detection of organophosphorus compounds

RECEIVED
22 October 2017

REVISED
27 January 2018

ACCEPTED FOR PUBLICATION
16 February 2018

PUBLISHED
16 March 2018

Minsu Kim[1], **Ji Eon Kwon**[2], **Kangwon Lee**[3,4] **and Won-Gun Koh**[1,4]

[1] Department of Chemical and Biomolecular Engineering, Yonsei University, 50 Yonsei-ro, Seodaemun-gu, Seoul 120-749, Republic of Korea
[2] Center for Supramolecular Optoelectronic Materials (CSOM), Research Institute of Advanced Materials (RIAM), Department of Materials Science and Engineering, Seoul National University, 1 Gwanak-ro, Gwanak-gu, Seoul 08826, Republic of Korea
[3] Program in Nanoscience and Technology, Graduate School of Convergence Science and Technology, Seoul National University, Seoul, Republic of Korea; Advanced Institutes of Convergence Technology, Gyeonggi-do, Republic of Korea
[4] Authors to whom any correspondence should be addressed.

E-mail: kangwonlee@snu.ac.kr **and** wongun@yonsei.ac.kr

Keywords: paraoxon biosensor, metal-enhanced fluorescence, hydrogel microarray, quantum dots, silica-coated silver nanoparticles

Supplementary material for this article is available online

Abstract

In this study, we developed an enzyme-based miniaturized fluorescence biosensor to detect paraoxon, one of the most well-known neurotoxic organophosphorus compounds. The biosensor was fabricated with poly(ethylene glycol) (PEG) hydrogel microarrays that entrapped acetylcholinesterase (AChE) and quantum dots (QDs) as fluorescence reporters. Metal-enhanced fluorescence (MEF) was utilized to amplify the fluorescence signal, which was achieved by decorating QDs on the surface of silica-coated silver nanoparticles (Ag@Silica). The MEF effects of Ag@Silica were optimized by tuning the thickness of the silica shells, and under the optimized conditions, the fluorescence intensity was shown to be increased 5 fold, compared with the system without MEF. PEG hydrogel microarray entrapping QD-decorated Ag@Silica and AChE was prepared via photopatterning process. The entrapped AChE hydrolyzed paraoxon to produce p-nitrophenol within the hydrogel microstructure, which subsequently quenched the fluorescence of the QDs on the surface of Ag@Silica. The MEF-assisted fluorescence detection resulted in a significant enhancement of paraoxon detection. The detection limit was approximately 1.0×10^{-10} M and 2.0×10^{-7} M for sensing with and without MEF, respectively. The successful integration of a hydrogel microarray system with a microfluidic system was demonstrated to be a potential application for the MEF-based micro-total-analysis-system.

1. Introduction

Organophosphorus compounds (OPs), which are routinely used as insecticides and chemical warfare agents, can be very harmful to humans when they are inhaled, intaken or absorbed through the skin [1]. OPs are known to inactivate acetylcholinesterase (AChE), which catalyzes the hydrolysis of acetylcholine (ACh). Therefore, inhibition of AChE causes ACh accumulation, which causes serious medical complications such as respiratory disorders, fibrillation and even can lead to death [2–5]. Due to the neurotoxicity of OPs, they need to be accurately monitored, and various analytical tools are used for the detection of OPs. These analytical methods include gas chromatography-mass spectroscopy [6], high performance liquid chromatography [7–9], and electrochemical sensors [10, 11]. Although these methods are sensitive and provide reliable analyzes for precise quantification, they are costly, time-consuming, and must be conducted by a skilled individual. Therefore, a lot of effort has been made to develop simple, accurate, sensitive and portable devices to detect OPs.

Enzyme-based biosensors using fluorescence have received attention for OP detection [12]. Fluorescence-based optical detection is very simple and provides reliable results. Optical transducers are not easily disturbed by reactions that take place in sample

solutions. Organophosphorus hydrolase (OPH) or AChE are commonly used as enzymatic probes, where fluorescence quenching resulting from the reaction between OPs and enzymes was monitored to detect OPs [13–15]. In spite of the numerous studies to develop fluorescence-based enzymatic biosensors for OP detection, few studies using microarrays or microfluidics have been reported. These techniques have the advantages of requiring a small volume of samples, high sensitivity, good reliability, and capability to detect multiple targets simultaneously [16].

Meanwhile, metal-enhanced fluorescence (MEF) is a phenomenon that takes place via electromagnetic coupling between localized surface plasmons of metal nanostructures and fluorescent materials. This process results in a significant amplification of the fluorescence emission intensity [17–20] and therefore, MEF-based fluorescence detection has been widely researched to enhance the performance of biosensors [21–24]. The level of the MEF effect is influenced by material factors such as size, shape and species of metal nanostructures as well as most importantly the distance between metal and fluorescence materials [25–29].

In this study, a MEF-based enzyme biosensor was developed using poly(ethylene glycol) (PEG) hydrogel microarrays that encapsulated the target receptor AChE and fluorescence reporter quantum dots (QDs). Paraoxon, one of the most well-known neurotoxins, was chosen as a model OP. Paraoxon produces p-nitrophenol (pNP) via reaction with AChE, which is an effective fluorescence quencher [30]. Therefore, detection of paraoxon can be monitored by amplified fluorescence quenching of QDs by MEF upon reaction. PEG hydrogel can entrap a large amount of AChE, in which entrapped enzymes are relatively safe against protein denaturation [31–33]. Transparency of PEG hydrogels is also potentially suitable for optical sensing of targets in biosensor applications. QDs were chosen as the signal reporter due to their excellent quantum efficiency, stability against photobleaching, and high sensitivity [34, 35]. To achieve MEF-assisted fluorescence detection of paraoxon, QDs were decorated onto the silica-coated silver nanoparticles (Ag@Silica). After preparation of the hydrogel microarray that encapsulated AChE and QD-decorated Ag@Silica, MEF-based biosensors were systematically investigated for their ability to improve the performance of fluorescence-based paraoxon detection using microarray and microfluidic systems.

2. Materials and methods

2.1. Materials

All reagents were purchased from Sigma-Aldrich (Milwaukee, WI, USA) unless otherwise noted. Poly (vinylpyrrolidone) (PVP, MW 10 000 Da) was purchased from Junsei Chemical Co., Ltd (Tokyo, Japan). A solution of 5 mg ml^{-1} carboxylated QDs in water (NSQDs-AC, emission wavelength 620 nm) was obtained from Nanosquare, Inc. (Seoul, Korea). Poly (dimethylsiloxane) (PDMS) elastomer was purchased as Dow Corning Sylgard 184 (Midland, MI, USA), which is composed of a prepolymer and curing agent. The photomask to create hydrogel micropattern was purchased from Advanced Reproductions (Andover, MA, USA).

2.2. Preparation of silica-coated silver nanoparticles

A polyol method, where PVP acts as a protecting and reducing agent, was used to obtain silver nanoparticles (AgNPs) [36]. Resultant AgNPs were coated with silica shell via the Stöber method [37], producing silica-coated AgNPs (Ag@Silica). Briefly, the 4 ml of AgNP solution in ethanol (1 mg ml^{-1}) underwent sonication for 10 min to minimize aggregation. Various amounts of tetraethyl orthosilicate (TEOS) were added to the AgNP solution under vigorous stirring to adjust the thickness of the silica shell. Then, the silica coating was initiated by adding 200 μl of an ammonium hydroxide solution to the AgNPs/TEOS colloid. The silica growth reaction was proceeded under continuous stirring overnight at 25 °C. Ag@Silica were then collected after multiple centrifugations and redispersed in ethanol.

2.3. Decoration of QD onto Ag@Silica

One hundred microliters of Ag@Silica (0.5 mg ml^{-1}) was dispersed in a 500 μl of a poly(ethyleneimine) (PEI, MW 750 000) (0.5 mg ml^{-1}) solution and reacted for 30 min with stirring. When the reaction was complete, Ag@Silica were washed twice and redispersed in 500 μl of DI water. 15 μl of a diluted QD solution (0.025 mg ml^{-1}) was added to the PEI-coated Ag@Silica solution and reacted with stirring for 10 min.

2.4. Nanoparticles characterization

Images of different nanoparticles were obtained by transmission electron microscope (TEM) (JEM-F200, JEOL Ltd Tokyo, Japan). Dynamic light scattering (DLS, Zetasizer 3000HSA, Malvern Instruments Ltd, Worcestershire, UK) was used to measure the size distribution of the nanoparticles. The absorbance of the nanoparticles was monitored using UV–vis–NIR Spectrophotometer (Agilent, Santa Clara, CA, USA).

2.5. Fabrication of hydrogel microarray

Hydrogel microarrays entrapping AChE and QD-decorated Ag@Silica (QD-Ag@Silica) were fabricated by photolithography as described in our previous studies [38, 39]. Briefly, precursor solution consisted of PEG diacrylate (PEG-DA, MW 575 Da) and 2-hydroxy-2-methylpropiophenone (HOMPP) as a photoinitiator. For the paraoxon detection, 100 μl of AChE (Type V-S, from Electrophorus electricus,

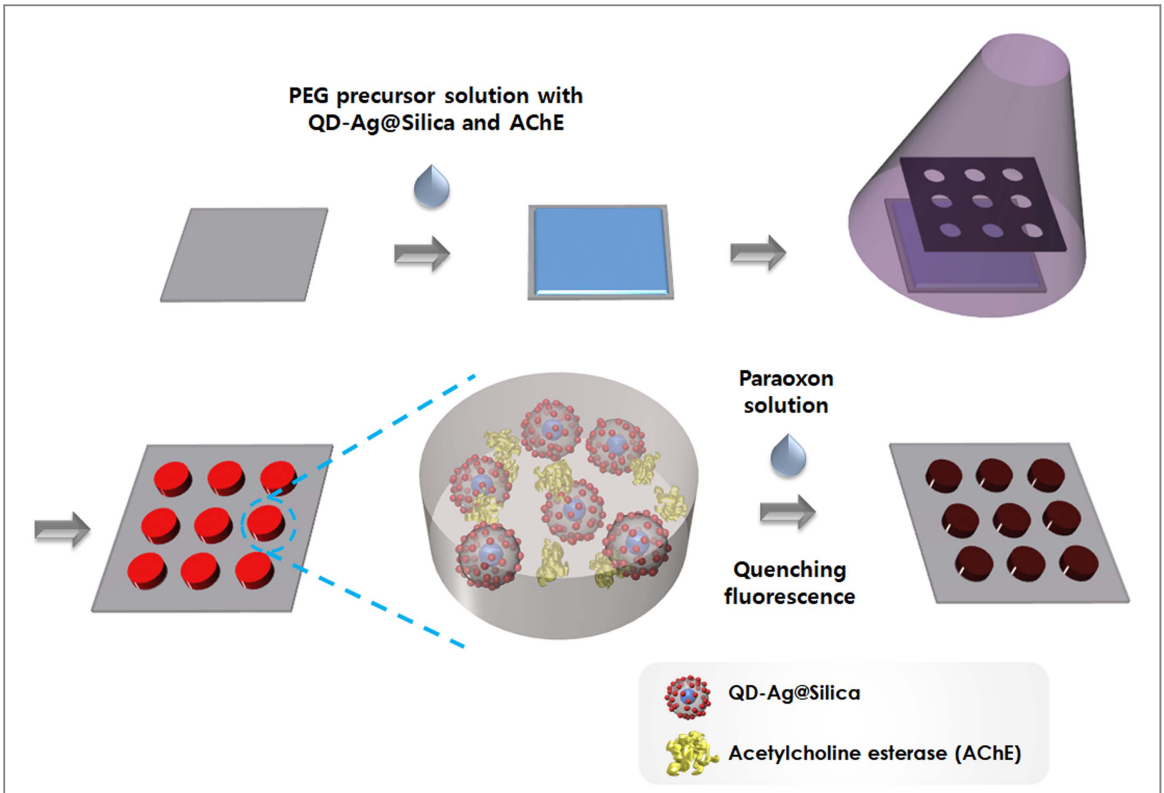

Figure 1. Schematic illustration of fabricating hydrogel microarrays entrapping QD-Ag@Silica and AChE for paraoxon detection.

1000 unit/mg protein) (0.1 μM, Tris-HCl buffer pH 7.4) was added to 1 ml of a precursor solution. QD-Ag@Silica was also included in the precursor solution to achieve MEF-based sensing. The resultant precursor solution underwent UV-induced photopatterning process, generating hydrogel microarray containing enzyme and QD-Ag@Silica on the glass substrate. The self-assembled monolayer of 3-(trichlorosilyl)propyl methacrylate (TPM) was incorporated onto glass surface to enhance the attachment of the hydrogel microstructure as previously described [40]. Figure 1 shows the fabrication process of the hydrogel micropatterns entrapping QD-Ag@Silica and AChE for the paraoxon detection.

2.6. Fabrication of the microfluidic device

PDMS-based microchannels that was irreversibly-sealed with glass slide was fabricated according to well-known method [41]. When hydrogel micropatterns were fabricated within the microfluidic system, microchannels filled with precursor solutions was exposed to UV light through a photomask for 1 s. The final hydrogel microstructures were produced inside the microchannels by removing unexposed precursor solution with multiple washing steps, which was achieved by injecting PBS solutions into microchannels using a syringe pump (Harvard Apparatus, Holliston, MA, USA).

2.7. Fluorescence detection

The reaction of AChE with paraoxon was first investigated in the solution state using a fluorescence spectrometer (Photon Technologies International, Monmouth, NJ, USA). Specifically, 100 μl of a 0.1 μM AChE solution in Tris-HCl buffer (pH 7.4) was mixed with QD-Ag@Silica or QD-Silica. After the addition of paraoxon solutions (900 μl, diluted with a pH 10 buffer) to the nanoparticle-containing AChE solution, the changes in the emission intensity resulted from the enzymatic reactions were observed at 620 nm. Time-resolved fluorescence lifetime experiments were performed through the time-correlated single photon counting methods by using a FluoTime 200 instrument (Picoquant, Berlin, Germany). A 377 nm diode laser with a repetition rate of 5 MHz was used as an excitation source. Fluorescence decay profiles were analyzed by FluoFit Pro software, using an exponential fitting model through deconvolution with the measured instrumental response function. For paraoxon detection inside the hydrogel, hydrogel microarrays entrapping AChE and QD-Ag@Silica or QD-Silica were reacted with paraoxon for 1 h. The change of fluorescent intensity from the hydrogel microarrays was monitored using a fluorescence microscopy (IX 71, Olympus, Tokyo, Japan). At least, five assays were carried out with each microarray to acquire the data.

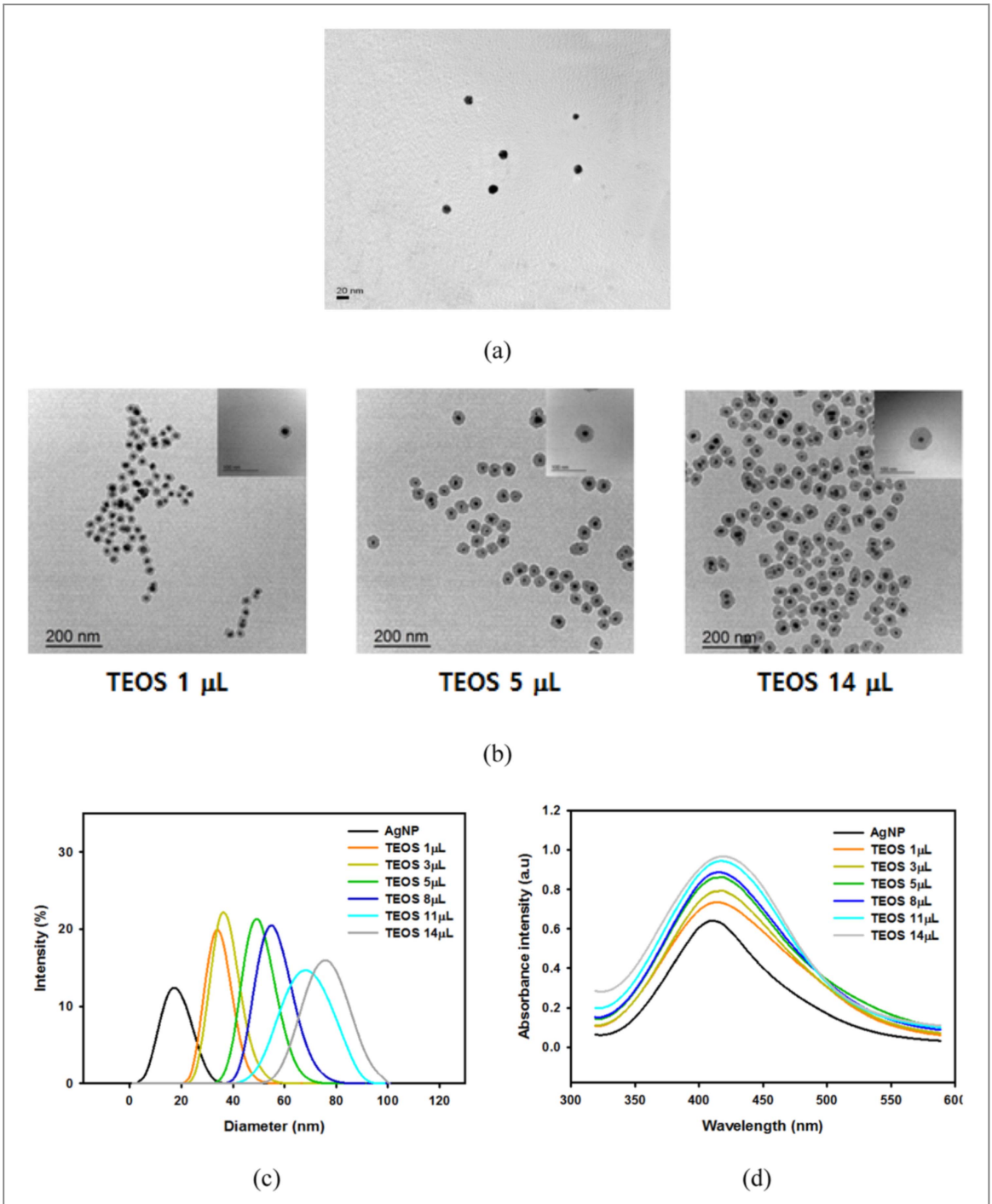

Figure 2. Preparation and characterization of Ag@Silica. (a) TEM image of bare AgNPs. (b) TEM images of Ag@Silica prepared with different amount of TEOS. (c) Size distribution and (d) absorbance spectra of Ag@Silica with different silica shell thickness.

3. Results

3.1. Characterization of nanoparticles

QD-Ag@Silica was used as a sensing element for MEF-based detection of paraoxon. First, AgNPs were synthesized using modified polyol process and TEM image shows that their diameter was approximately 20 nm (figure 2(a)). The resultant AgNPs were coated with silica shells through the Stöber method, as shown in figure 2(b). The thickness of the silica shell was controlled by the amount of TEOS, where thicker silica layers were formed with increasing TEOS (figure 2(b)). The MEF effect of the metal nanostructures on the QDs strongly depended on the distance between the metal and QDs [42, 43]. At very close contact (<10 nm), fluorescence quenching became dominant over fluorescence amplification because of the resonance energy transfer between the metal nanoparticles and excited QDs [44]. On the other hands, when the distance between the fluorophore and metal was longer than the effective plasmonic penetration depth of the metal nanoparticles, neither the quenching nor the fluorescent amplification effect was observed. Therefore, the control of distance

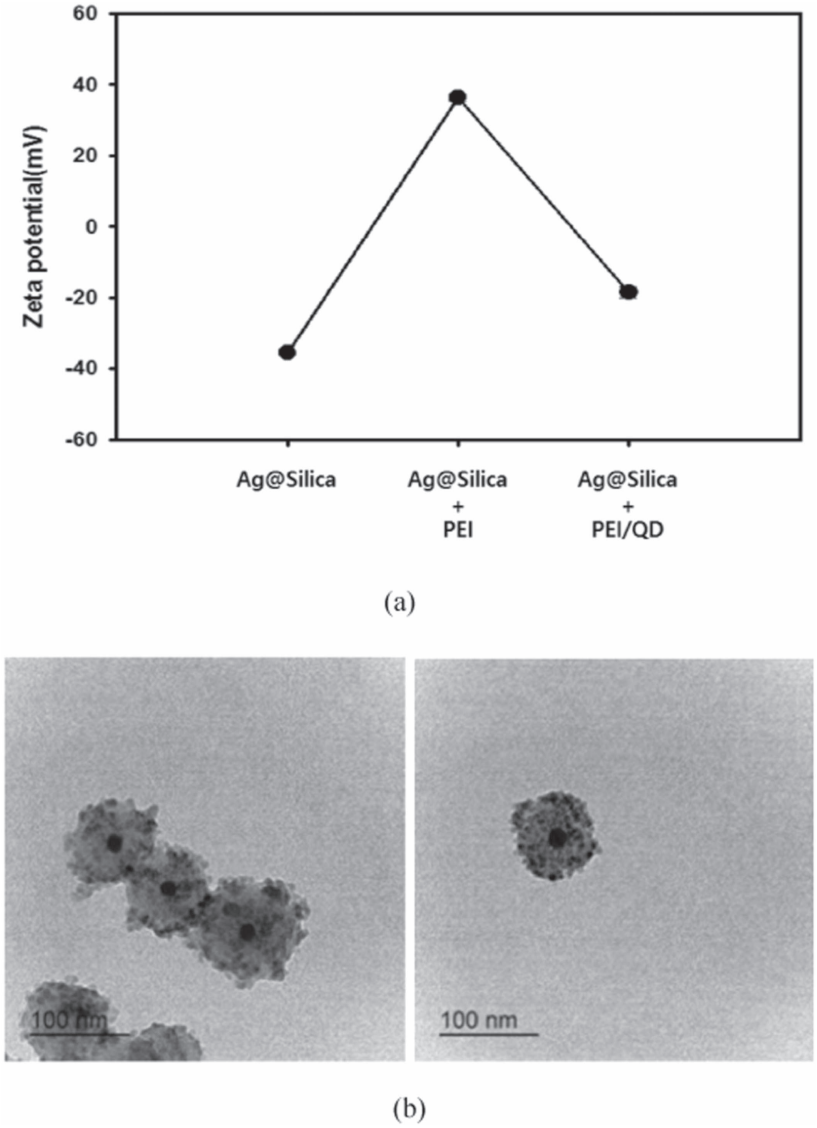

Figure 3. Decoration of Ag@Silica with QDs. (a) Change of zeta potential of Ag@Silica after deposition of PEI and QD. (b) TEM image of QD-decorated Ag@Silica.

between them is the key factor for maximizing the MEF phenomenon. Here, passivation of silver with silica shell played an important role as a spacer between AgNP and QD to achieve the maximum sensing efficiency through the MEF effect [45]. The change of the particle size as a function of the amount of TEOS was also analyzed through DLS, as shown in figure 2(c). The average silica shell thicknesses were 8.1, 10.1, 15.7, 19.2, 25.8, 29.9 nm when AgNPs were reacted with 1, 3, 5, 8, 11 and 14 μl of TEOS, respectively. The generation of Ag@Silica was also confirmed by monitoring the absorbance. The surface plasmon resonance (SPR) peak of AgNPs was narrow at 415 nm. However, the absorbance peaks of Ag@Silica were red-shifted with the increasing silica shell thickness (figure 2(d)). The resultant Ag@Silica were decorated with QDs via an electrostatic interaction. Since both Ag@Silica and carboxylated QDs had negative charges, positively charged PEI was deposited on the silica layer and then QDs were successfully attached to PEI-coated Ag@Silica. The zeta potential measurement demonstrated the successful deposition of positive PEI and negative QDs (figure 3(a)). The TEM image (figure 3(b)) shows QD-decorated Ag@Silica (QD-Ag@Silica).

3.2. Optimization of MEF effect

The MEF effect of Ag@Silica on the decorated QDs was first monitored by changing the silica shell thickness. Here, the fluorescence intensity of QDs decorated on the bare silica nanoparticles (QD-Silica) was used as the control value. Figure 4(a) shows that the more significant MEF effect was obtained by increasing the thickness of the silica layer, and the fluorescence intensity reached the maximum value when the thickness of the silica layer was 19.2 $\pm$ 1.55 nm. The fluorescence enhancement factor (ratio of fluorescence intensity with MEF to

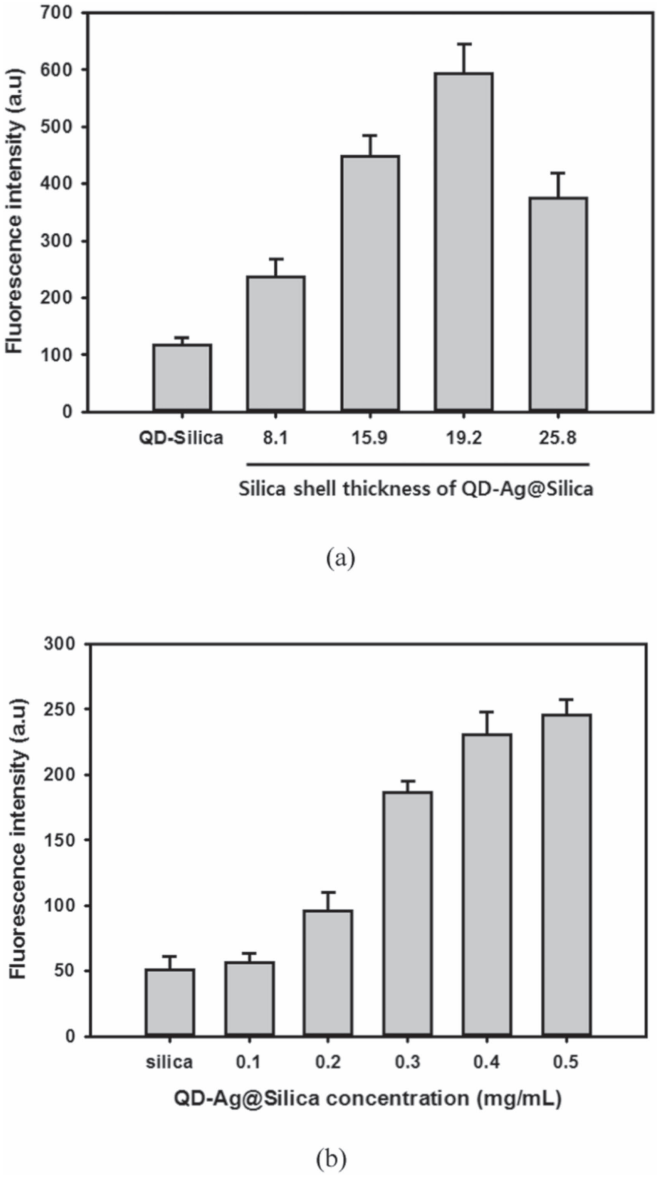

Figure 4. Optimization of fluorescence emission intensity of QD-Ag@Silica. (a) MEF effect of Ag@Silica on the QDs as a function of silica shell thickness. (b) Change of fluorescence intensity according to QD-Ag@Silica concentration.

without MEF) was approximately 5 under this condition. When the silica layer was thicker than 19.2 nm, the extent of the fluorescence enhancement decreased. This was because less SPR energy from the silver nanoparticles was transferred to the QDs, which resulted in the decrease of the coupling reaction between QDs and AgNPs. The fluorescence intensity also increased with the amount of QD-Ag@Silica up to 0.5 mg ml^{-1} as shown in figure 4(b). However, further enhancement was not achieved when the concentration of QD-Ag@Silica was greater than 0.5 mg ml^{-1}. Based on these results, we used QD-Ag@Silica with a 19.2 nm silica shell (0.5 mg ml^{-1}) for the rest of the experiments. The origin of the MEF effect was further elucidated by fluorescence lifetime measurements. As shown in fluorescence decay curve (figure S1 and table S1 in supplementary data are available online at stacks.iop.org/BF/10/035002/mmedia), we clearly observed the reduction in average fluorescence lifetime (t_{avg} 2.55 ns → 1.99 ns) in silver-containing nanoparticles.

3.3. Paraoxon assay in solution state

The main principle for the paraoxon detection is fluorescence quenching of QDs by p-nitrophenol (pNP), which is a hydrolytic product that forms from the reaction between AChE and paraoxon, as described in figure 5(a) [46]. To confirm the detection mechanism, different concentrations of paraoxons were reacted with AChE in QD-Silica (without MEF) and QD-Ag@Silica (with MEF) solution. The resulting fluorescence spectra were recorded, as shown in figure 5(b). More fluorescence quenching was observed with the increase of paraoxon concentration in both cases. These results proved that the AChE-catalyzed reaction with paraoxon produced pNP,

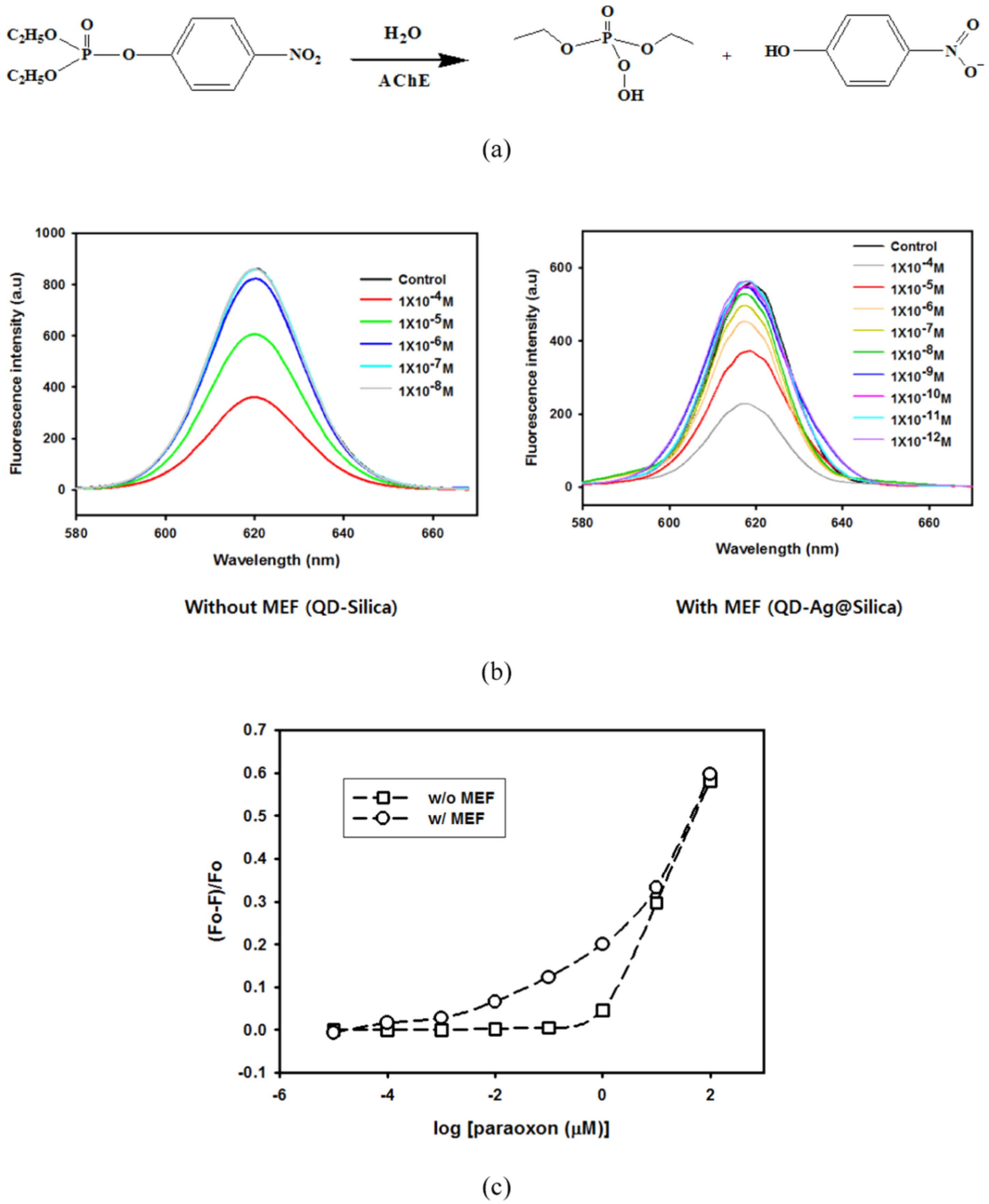

Figure 5. Investigation of the reaction between paraoxon and AChE in solution by monitoring the fluorescence quenching of QDs. (a) Scheme of the reaction between paraoxon and AChE that produce pNP (quencher of QD). (b) Change of fluorescence spectra after the reaction between AChE and different concentration of paraoxon with and without MEF effect. (c) Change of $(F_0 - F)/F_0$ value as a function of paraoxon concentration.

which led to quenching of the QD emission. However, the difference between two systems become obvious in figure 5(c) that shows the change of $(F_0 - F)/F_0$ value as a function of paraoxon concentration (F: quenched fluorescence intensity after the reaction, F_0: fluorescence intensity before the reaction). Here, the amplified $(F_0 - F)/F_0$ value at low concentrations was clearly shown in the hydrogel microarray containing QD-Ag@Silica due to the MEF phenomenon. Both systems had similar $(F_0 - F)/F_0$ value at high concentration of paraoxon up to 10^{-5} M but the different became significant at lower concentration of paraoxon. Without MEF effect (QD-Silica system), paraoxon below 10^{-7} M could not be detected, while even 10^{-9} M was detected with MEF effect (QD-Ag@Silica system).

3.4. Paraoxon detection within hydrogel microarrays

After confirming that the QDs decorated on Ag@Silica represent a better fluorescence probe for paraoxon detection than normal QDs due to the MEF effect, hydrogel microarrays containing QD-Ag@Silica and

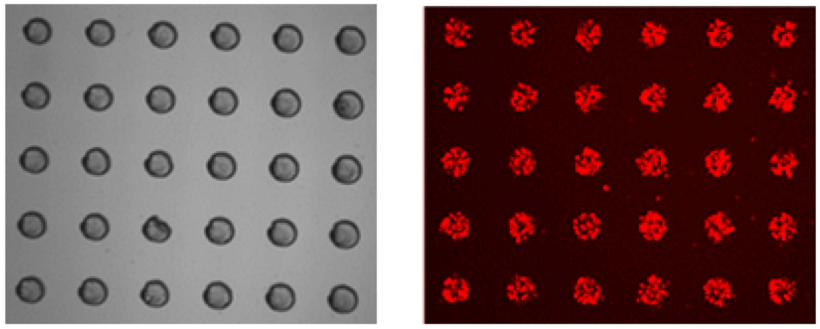

(a)

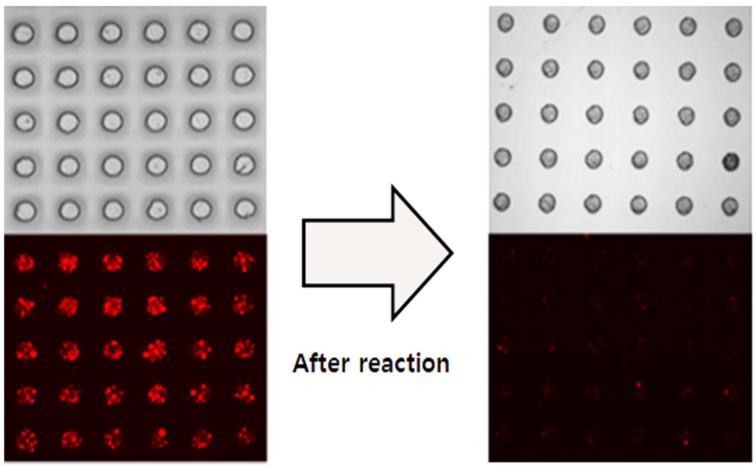

(b)

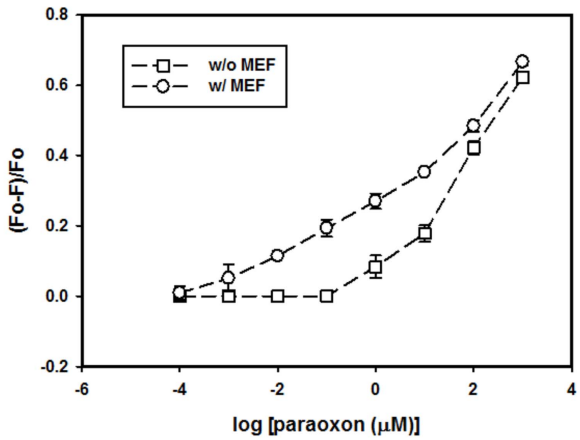

(c)

Figure 6. Detection of paraoxon using hydrogel microarrays entrapping QD-Ag@Silica and AChE. (a) Optical and fluorescence images of hydrogel microarrays. (b) Change of fluorescence intensity of hydrogel microarray after the reaction between AChE and paraoxon. (c) Change of $(F_0 - F)/F_0$ value as a function of paraoxon concentration.

AChE were prepared for paraoxon detection. The capability of PEG-DA to be photopatterned via simple photolithography process was utilized to generate a hydrogel micropattern with a 100 μm diameter. Figure 6(a) shows that well-defined hydrogel microarray was fabricated on the glass substrate. Furthermore, fluorescence was observed only in the hydrogel micropattern, which demonstrated that QD-Ag@Silica were successfully entrapped inside the hydrogel microstructures and unexposed precursor solution was completely washed away by developing step. The resultant hydrogel microarrays were utilized for the detection of paraoxon based on the same principle explained earlier, except that all of the reactions only

(a)

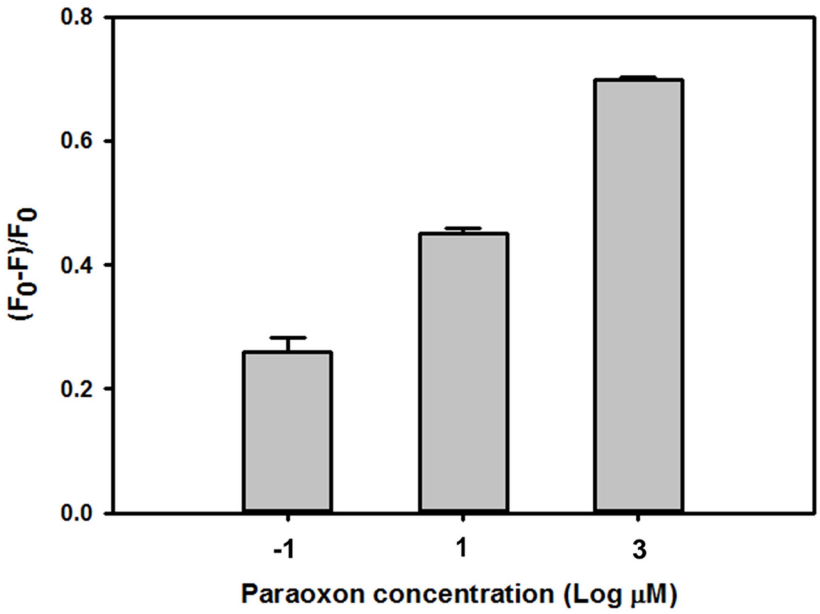

(b)

Figure 7. Incorporation of hydrogel microarray into microfluidic system. (a) Optical and fluorescence images of hydrogel microarrays within a microchannel that were exposed to different concentration of paraoxon. (b) Change of $(F_0 - F)/F_0$ value as a function of three different paraoxon concentrations.

occurred inside the hydrogel. That is, paraoxon can diffuse into a hydrogel microarray and react with AChE to produce a pNP that quenches the QDs on Ag@Silica within the hydrogel. Figure 6(b) shows the fluorescence images of a hydrogel microarray entrapping QD-Ag@Silica and AChE before and after reaction with paraoxon. The hydrogel microarrays that reacted with paraoxon emitted weaker fluorescence signals than those prior to the reaction because of the quenching of QDs by the pNP generated through the reaction between AChE and paraoxon within the hydrogel microstructures. Next, quantitative analysis of paraoxon was performed by reacting hydrogel microarrays with different concentrations of paraoxon. Similar trends were observed for the values of $(F_0 - F)/F_0$ with the results obtained in solution for both hydrogel microarrays encapsulating QD-Ag@Silica and QD-Silica (figure 6(c)). Therefore, figure 6(c) shows that the $(F_0 - F)/F_0$ values decreased as the paraoxon concentration decreased. However, hydrogel microarray encapsulating QD-Ag@Silica showed better performance in terms of detection limit. The detection limit of MEF-based system was three orders of magnitude lower than that of the other system without MEF effect. The detection limit was approximately 4.0×10^{-10} M and 2.0×10^{-7} M for sensing with and without MEF, respectively

Finally, the feasibility of using hydrogel microstructures entrapping QD-Ag@Silica and AChE for paraoxon detection was demonstrated within

Table 1. Performance comparison of paraoxon biosensors based on fluorescence detection.

Used enzyme	Detection scheme	Assay system	Enzyme concentration	Detection limit	Reference
AChE and ChOx	Quenching of QD by H_2O_2	Solution-based	0.0002 mg ml^{-1}	1.0×10^{-12} M	[47]
AChE and ChOx	Quenching of d-dot by H_2O_2	Solution-based	0.004 mg ml^{-1}	1.31×10^{-11} M	[48]
AChE and ChOx	Quenching of QD by H_2O_2	Multilayer film	0.5 mg ml^{-1}	2.75×10^{-12} M	[49]
AChE	Quenching of dialkylcoumarin by pNP + enzyme inhibition	Solution-based	0.0002 mg ml^{-1}	3.5×10^{-12} M	[46]
OPH	Fluorescence quenching of a Coumarin derivative by pNP	Solution-based	0.001 mg ml^{-1}	7.0×10^{-7} M	[30]
OPH	Quenching of QD by secondary structure change	Solution-based	0.003 mg ml^{-1}	1.0×10^{-8} M	[13]
OPH	FITC fluorescence quenching by pNP	LB film	0.18 mg ml^{-1}	1.0×10^{-9} M	[51]
OPH	Intensity change of pH-sensitive fluorophore	Solution-based	0.4 mg ml^{-1}	7.0×10^{-12} M	[52]
OPH	Intensity change of pH-sensitive fluorophore	Solution-based	1 mg ml^{-1}	1.0×10^{-6} M	[53]
AChE	Quenching of QD by pNP	Hydrogel microarray	0.025 mg ml^{-1}	4.0×10^{-10} M	This study

microfluidic systems. Figure 7(a) shows optical and fluorescent images of the hydrogel microarrays entrapping AChE/QD-Ag@Silica or AChE/QD-Silica fabricated in different microchannels, which were then reacted with paraoxon. Fluorescence intensity decreased as injected paraoxon concentration increased. Figure 7(b) shows quantitative data of $(F_0 - F)/F_0$ values from hydrogel microarrays as a function of paraoxon concentration inside the microchannels, demonstrating that microfluidic-based paraoxon sensing is possible using developed detection system.

4. Discussion

Conventionally, methods for fluorescence detection of paraoxon using enzyme-based biosensor are categorized into two groups depending on the number of enzymes used in the assays. In first approach, paraoxon was detected via bi-enzymatic reaction using two different enzymes, AChE and choline oxidase (ChOx). The enzymatic reaction between AChE and ACh produced choline, which was subsequently oxidized by ChOx to produce hydrogen peroxide. Hydrogen peroxide can quench the fluorescence of various organic and inorganic fluorophore. Since paraoxon is inhibitor of the first enzymatic reaction, introduction of paraoxon eventually decreases the production of hydrogen peroxide and changes the extent of fluorescence quenching [47–50]. Therefore, paraoxon concentration can be determined by monitoring the change of fluorescence quenching. Although bi-enzymatic analysis methods result in superior sensing performance (detection limit ranges from 10^{-10} to 10^{-12} M, table 1), there is a problem in price because two enzymes are used, and there is another problem that the enzyme activity or/and immobilization must be optimized for both enzyme simultaneously. In second approach, only one enzyme such as OPH or AChE was used for paraoxon sensing. These enzymes can catalyze the hydrolysis of paraoxon, generating pNP and protons. The former quenches the fluorescence of organic fluorescence dye or QDs, while the letter changes the local pH. Therefore, paraoxon can be monitored by measuring the change of fluorescence quenching or intensity change of pH-sensitive fluorophores [13, 30, 46, 51–53]. The paraoxon detection using one enzyme is advantageous in terms of simple and cost-effective experimental procedure, but its sensitivity is lower than bi-enzymatic assays (detection limit ranges from 10^{-6} to 10^{-12} M, table 1). Although few systems were developed on solid support as film types using layer-by-layer or Langmuir–Blodgett (LB) deposition [49, 51, 54], most of fluorescence sensing of paraoxon (both one and two enzyme system) was carried out in solution state using free or nanoparticle-immobilized enzymes. However, for more useful bioassay system such as microarray or microfluidic-based biosensor, enzymes immobilized onto solid supports were more preferred to suspended enzymes in solution. In this study, we developed one enzyme-based paraoxon sensor which can be fabricated in the form of a microarray and be integrated into microfluidic system. PEG hydrogel was used as an enzyme immobilization matrix, where AChE was entrapped by photocrosslinking and maintained the activity. Low sensitivity associated with using hydrogel-entrapped one enzyme was overcome by employing MEF effect. According to previous study [55], mesh size of PEG hydrogel was approximately 10 Å, which is larger than the size of paraoxon and smaller than the size of AChE. Therefore, the crosslinking density of hydrogel was dense enough to prevent entrapped enzyme from diffusing out and loose enough to allow the penetration of paraoxon. QDs were used as a fluorescence reporter and MEF was achieved by decorating QDs onto the Ag@Silica. Most of MEF-based biosensors were prepared on two-dimensional rigid substrate or on nanoparticle suspended in solution, both of which can cause the denature of proteins or difficulties in miniaturizing [56–59]. We expected that the use of hydrogel as a MEF sensing platform can overcome those problems related with suspension or 2D-based system due to soft and hydrated nature of hydrogels. After optimizing the MEF effect, hydrogel microarray entrapping AChE and QD-Ag@Silica was fabricated on glass substrates and within microchannels. With the help of MEF effect, we were able to develop the paraoxon biosensor with similar performance to previously-reported biosensor. The comparison between our proposed MEF-based sensing and several other fluorescence paraoxon biosensors was summarized in table 1. It was reported that the higher the concentration of AChE, the more pNP was produced during the same reaction time, which could enhance the detection limit of paraoxon biosensor [46, 48]. Although our hydrogel-immobilized system used higher concentration of AChE than solution-based assay, it is much lower than other immobilized system such as multilayer or LB film.

5. Conclusion

In summary, a fast and readily applicable strategy was established to develop a QD-based fluorescence hydrogel microarray for detecting toxic OPs chemicals that cause nervous system disorders. Paraoxon, as a target model, was utilized to investigate the proposed QD-based biosensor systematically. MEF was adopted to improve the biosensor performance by decorating QDs on the surface of Ag@Silica. MEF effect was optimized by controlling the distance between QD and silver nanoparticles using the silica layer, which resulted in a significant enhancement of fluorescence intensity from the QDs. Paraoxon was detected based on amplified fluorescence quenching upon exposure

to pNP that was produced by AChE-catalyzed hydrolytic reactions. The sensitivities of MEF-assisted biosensor are over three orders of magnitude higher than those without MEF effect. MEF-based paraoxon biosensing was successfully carried out not only in the solution state but also within the hydrogel microarrays as well as within microfluidic systems.

Acknowledgments

This work was supported by the National Research Foundation of Korea (NRF) grant funded by the Korea government (MSIP) (NRF-2017M3D1A1039289, 2017M3A7B4041798, 2009-0093823, 2016R1D1A1B03932220, and 2017M3A7B4049850)

ORCID iDs

Won-Gun Koh https://orcid.org/0000-0002-5191-2531

References

[1] Zhang T, Zeng L, Han L, Li T, Zheng C, Wei M and Liu A 2014 Ultrasensitive electrochemical sensor for p-nitrophenyl organophosphates based on ordered mesoporous carbons at low potential without deoxygenization *Anal. Chim. Acta* **822** 23–9

[2] Gong J, Miao X, Zhou T and Zhang L 2011 An enzymeless organophosphate pesticide sensor using Au nanoparticle-decorated graphene hybrid nanosheet as solid-phase extraction *Talanta* **85** 1344–9

[3] Chen Y 2012 Organophosphate-induced brain damage: mechanisms, neuropsychiatric and neurological consequences, and potential therapeutic strategies *Neurotoxicology* **33** 391–400

[4] Du D, Wang J, Smith J N, Timchalk C and Lin Y 2009 Biomonitoring of organophosphorus agent exposure by reactivation of cholinesterase enzyme based on carbon nanotube-enhanced flow-injection amperometric detection *Anal. Chem.* **81** 9314–20

[5] Hossain S Z, Luckham R E, McFadden M J and Brennan J D 2009 Reagentless bidirectional lateral flow bioactive paper sensors for detection of pesticides in beverage and food samples *Anal. Chem.* **81** 9055–64

[6] Zacharis C K, Christophoridis C and Fytianos K 2012 Vortex-assisted liquid–liquid microextraction combined with gas chromatography-mass spectrometry for the determination of organophosphate pesticides in environmental water samples and wines *J. Sep. Sci.* **35** 2422–9

[7] He L, Luo X, Jiang X and Qu L 2010 A new 1, 3-dibutylimidazolium hexafluorophosphate ionic liquid-based dispersive liquid–liquid microextraction to determine organophosphorus pesticides in water and fruit samples by high-performance liquid chromatography *J. Chromatogr.* A **1217** 5013–20

[8] Wu C, Liu H, Liu W, Wu Q, Wang C and Wang Z 2010 Determination of organophosphorus pesticides in environmental water samples by dispersive liquid–liquid microextraction with solidification of floating organic droplet followed by high-performance liquid chromatography *Anal. Bioanal. Chem.* **397** 2543–9

[9] Li L, Zhou S, Jin L, Zhang C and Liu W 2010 Enantiomeric separation of organophosphorus pesticides by high-performance liquid chromatography, gas chromatography and capillary electrophoresis and their applications to environmental fate and toxicity assays *J. Chromatogr.* B **878** 1264–76

[10] Llopis X, Ibáñez-García N, Alegret S and Alonso J 2007 Pesticide determination by enzymatic inhibition and amperometric detection in a low-temperature cofired ceramics microsystem *Anal. Chem.* **79** 3662–6

[11] Privett B J, Shin J H and Schoenfisch M H 2008 Electrochemical sensors *Anal. Chem.* **80** 4499–517

[12] Ispas C R, Crivat G and Andreescu S 2012 Recent developments in enzyme-based biosensors for biomedical analysis *Anal. Lett.* **45** 168–86

[13] Ji X, Zheng J, Xu J, Rastogi V K, Cheng T-C, DeFrank J J and Leblanc R M 2005 (CdSe) ZnS quantum dots and organophosphorus hydrolase bioconjugate as biosensors for detection of paraoxon *J. Phys. Chem.* B **109** 3793–9

[14] Tuteja S K, Kukkar M, Kumar P, Paul A and Deep A 2014 Synthesis and characterization of silica-coated silver nanoprobe for paraoxon pesticide detection *BioNanoScience* **4** 149–56

[15] Obare S O, De C, Guo W, Haywood T L, Samuels T A, Adams C P, Masika N O, Murray D H, Anderson G A and Campbell K 2010 Fluorescent chemosensors for toxic organophosphorus pesticides: a review *Sensors* **10** 7018–43

[16] Heo J and Crooks R M 2005 Microfluidic biosensor based on an array of hydrogel-entrapped enzymes *Anal. Chem.* **77** 6843–51

[17] Geddes C D and Lakowicz J R 2002 Metal-enhanced fluorescence *J. Fluoresc.* **12** 121–9

[18] Aslan K, Lakowicz J R and Geddes C D 2005 Rapid deposition of triangular silver nanoplates on planar surfaces: application to metal-enhanced fluorescence *J. Phys. Chem.* B **109** 6247–51

[19] Kulakovich O, Strekal N, Yaroshevich A, Maskevich S, Gaponenko S, Nabiev I, Woggon U and Artemyev M 2002 Enhanced luminescence of CdSe quantum dots on gold colloids *Nano Lett.* **2** 1449–52

[20] Pompa P, Martiradonna L, Della Torre A, Della Sala F, Manna L, De Vittorio M, Calabi F, Cingolani R and Rinaldi R 2006 Metal-enhanced fluorescence of colloidal nanocrystals with nanoscale control *Nat. Nanotechnol.* **1** 126–30

[21] Pang Y, Rong Z, Wang J, Xiao R and Wang S 2015 A fluorescent aptasensor for H5N1 influenza virus detection based-on the core–shell nanoparticles metal-enhanced fluorescence (MEF) *Biosens. Bioelectron.* **66** 527–32

[22] Petryayeva E and Krull U J 2011 Localized surface plasmon resonance: nanostructures, bioassays and biosensing—a review *Anal. Chim. Acta* **706** 8–24

[23] Sui N, Wang L, Yan T, Liu F, Sui J, Jiang Y, Wan J, Liu M and William W Y 2014 Selective and sensitive biosensors based on metal-enhanced fluorescence *Sensors Actuators* B **202** 1148–53

[24] Bauch M, Toma K, Toma M, Zhang Q and Dostalek J 2014 Plasmon-enhanced fluorescence biosensors: a review *Plasmonics* **9** 781–99

[25] Zhang J, Fu Y, Chowdhury M H and Lakowicz J R 2008 Single-molecule studies on fluorescently labeled silver particles: effects of particle size *J. Phys. Chem.* C **112** 18–26

[26] Bardhan R, Grady N K and Halas N J 2008 Nanoscale control of near-infrared fluorescence enhancement using Au nanoshells *Small* **4** 1716–22

[27] Bardhan R, Grady N K, Cole J R, Joshi A and Halas N J 2009 Fluorescence enhancement by Au nanostructures: nanoshells and nanorods *ACS Nano* **3** 744–52

[28] Magnan F, Gagnon J, Fontaine F-G and Boudreau D 2013 Indium@silica core–shell nanoparticles as plasmonic enhancers of molecular luminescence in the UV region *Chem. Commun.* **49** 9299–301

[29] Ayala-Orozco C, Liu J G, Knight M W, Wang Y, Day J K, Nordlander P and Halas N J 2014 Fluorescence enhancement of molecules inside a gold nanomatryoshka *Nano Lett.* **14** 2926–33

[30] Paliwal S, Wales M, Good T, Grimsley J, Wild J and Simonian A 2007 Fluorescence-based sensing of p-nitrophenol and p-nitrophenyl substituent organophosphates *Anal. Chim. Acta* **596** 9–15

[31] Ikami M, Kawakami A, Kakuta M, Okamoto Y, Kaji N, Tokeshi M and Baba Y 2010 Immuno-pillar chip: a new platform for rapid and easy-to-use immunoassay *Lab Chip* **10** 3335–40
[32] Kiyonaka S, Sada K, Yoshimura I, Shinkai S, Kato N and Hamachi I 2004 Semi-wet peptide/protein array using supramolecular hydrogel *Nat. Mater.* **3** 58
[33] Lee W, Choi D, Kim J-H and Koh W-G 2008 Suspension arrays of hydrogel microparticles prepared by photopatterning for multiplexed protein-based bioassays *Biomed. Microdevices* **10** 813–22
[34] Bruchez M, Moronne M, Gin P, Weiss S and Alivisatos A P 1998 Semiconductor nanocrystals as fluorescent biological labels *Science* **281** 2013–6
[35] Chan W C and Nie S 1998 Quantum dot bioconjugates for ultrasensitive nonisotopic detection *Science* **281** 2016–8
[36] Zhang F, Braun G B, Shi Y, Zhang Y, Sun X, Reich N O, Zhao D and Stucky G 2010 Fabrication of Ag@SiO_2@Y_2O_3: Er nanostructures for bioimaging: tuning of the upconversion fluorescence with silver nanoparticles *J. Am. Chem. Soc.* **132** 2850–1
[37] Aslan K, Wu M, Lakowicz J R and Geddes C D 2007 Fluorescent core–shell Ag@SiO_2 nanocomposites for metal-enhanced fluorescence and single nanoparticle sensing platforms *J. Am. Chem. Soc.* **129** 1524–5
[38] Jang E, Kim M and Koh W-G 2015 Ag@SiO_2-entrapped hydrogel microarray: a new platform for a metal-enhanced fluorescence-based protein assay *Analyst* **140** 3375–83
[39] Jang E, Son K J, Kim B and Koh W-G 2010 Phenol biosensor based on hydrogel microarrays entrapping tyrosinase and quantum dots *Analyst* **135** 2871–8
[40] Revzin A, Russell R J, Yadavalli V K, Koh W-G, Deister C, Hile D D, Mellott M B and Pishko M V 2001 Fabrication of poly (ethylene glycol) hydrogel microstructures using photolithography *Langmuir* **17** 5440–7
[41] Duffy D C, McDonald J C, Schueller O J and Whitesides G M 1998 Rapid prototyping of microfluidic systems in poly (dimethylsiloxane) *Anal. Chem.* **70** 4974–84
[42] Ray K, Badugu R and Lakowicz J R 2006 Distance-dependent metal-enhanced fluorescence from Langmuir–Blodgett monolayers of Alkyl-NBD derivatives on silver island films *Langmuir* **22** 8374–8
[43] Ray K, Badugu R and Lakowicz J R 2007 Polyelectrolyte layer-by-layer assembly to control the distance between fluorophores and plasmonic nanostructures *Chem. Mater.* **19** 5902–9
[44] Zhang Y, Dragan A and Geddes C D 2009 Wavelength dependence of metal-enhanced fluorescence *J. Phys. Chem.* C **113** 12095–100
[45] Ribeiro T, Baleizão C and Farinha J P S 2017 Artefact-free evaluation of metal enhanced fluorescence in silica coated gold nanoparticles *Sci. Rep.* **7** 2440
[46] Wang K, Wang L, Jiang W and Hu J 2011 A sensitive enzymatic method for paraoxon detection based on enzyme inhibition and fluorescence quenching *Talanta* **84** 400–5
[47] Ban R, Zhu J-J and Zhang J 2014 Manganese-doped ZnS quantum dots as a phosphorescent probe for use in the bi-enzymatic determination of organophosphorus pesticides *Microchim. Acta* **181** 1591–9
[48] Gao X, Tang G and Su X 2012 Optical detection of organophosphorus compounds based on Mn-doped ZnSe d-dot enzymatic catalytic sensor *Biosens. Bioelectron.* **36** 75–80
[49] Zheng Z, Li X, Dai Z, Liu S and Tang Z 2011 Detection of mixed organophosphorus pesticides in real samples using quantum dots/bi-enzyme assembly multilayers *J. Mater. Chem.* **21** 16955–62
[50] Zheng Z, Zhou Y, Li X, Liu S and Tang Z 2011 Highly-sensitive organophosphorous pesticide biosensors based on nanostructured films of acetylcholinesterase and CdTe quantum dots *Biosens. Bioelectron.* **26** 3081–5
[51] Cao X, Mello S V, Leblanc R M, Rastogi V K, Cheng T-C and DeFrank J J 2004 Detection of paraoxon by immobilized organophosphorus hydrolase in a Langmuir–Blodgett film *Colloids Surf.* A **250** 349–56
[52] Thakur S, Kumar P, Reddy M V, Siddavattam D and Paul A 2013 Enhancement in sensitivity of fluorescence based assay for organophosphates detection by silica coated silver nanoparticles using organophosphate hydrolase *Sensors Actuators* B **178** 458–64
[53] Viveros L, Paliwal S, McCrae D, Wild J and Simonian A 2006 A fluorescence-based biosensor for the detection of organophosphate pesticides and chemical warfare agents *Sensors Actuators* B **115** 150–7
[54] Xue G, Yue Z, Bing Z, Yiwei T, Xiuying L and Jianrong L 2016 Highly-sensitive organophosphorus pesticide biosensors based on CdTe quantum dots and bi-enzyme immobilized eggshell membranes *Analyst* **141** 1105–11
[55] Russell R, Axel A, Shields K and Pishko M 2001 Mass transfer in rapidly photopolymerized poly (ethylene glycol) hydrogels used for chemical sensing *Polymer* **42** 4893–901
[56] Aslan K, Gryczynski I, Malicka J, Matveeva E, Lakowicz J R and Geddes C D 2005 Metal-enhanced fluorescence: an emerging tool in biotechnology *Curr. Opin. Biotechnol.* **16** 55–62
[57] Aslan K, Wu M, Lakowicz J R and Geddes C D 2007 Metal enhanced fluorescence solution-based sensing platform 2: fluorescent core–shell Ag@SiO_2 nanoballs *J. Fluoresc.* **17** 127–31
[58] Hu P P, Zheng L L, Zhan L, Li J Y, Zhen S J, Liu H, Luo L F, Xiao G F and Huang C Z 2013 Metal-enhanced fluorescence of nano-core–shell structure used for sensitive detection of prion protein with a dual-aptamer strategy *Anal. Chim. Acta* **787** 239–45
[59] Wei X, Li H, Li Z, Vuki M, Fan Y, Zhong W and Xu D 2012 Metal-enhanced fluorescent probes based on silver nanoparticles and its application in IgE detection *Anal. Bioanal. Chem.* **402** 1057–63